Review

Cell PRESS

# Artificial molecular sieves and filters: a new paradigm for biomolecule separation

Jianping Fu[1,2], Pan Mao[3] and Jongyoon Han[2,4]

[1] Research Laboratory of Electronics, Massachusetts Institute of Technology, Cambridge, MA 02139, USA
[2] Department of Electrical Engineering and Computer Science, Massachusetts Institute of Technology, Cambridge, MA 02139, USA
[3] Department of Mechanical Engineering, Massachusetts Institute of Technology, Cambridge, MA 02139, USA
[4] Department of Biological Engineering, Massachusetts Institute of Technology, Cambridge, MA 02139, USA

**Patterned regular sieves and filters with comparable molecular dimensions hold great promise as an alternative to conventional polymeric gels and fibrous membranes to improve biomolecule separation. Recent developments of microfabricated nanofluidic sieves and filters have demonstrated superior performance for both analytical and preparative separation of various physiologically relevant macromolecules, including proteins. The insights gained from designing these artificial molecular sieves and filters, along with the promising results gathered from their first applications, serve to illustrate the impact that they can have on improving future separation of complex biological samples. Further development of artificial sieves and filters with more elaborate geometrical constraints and tailored surface functionality is believed to provide more promising ideals and results for biomolecule separation, which has great implications for proteomic research and biomarker discovery.**

## Introduction

In modern biology and biomedical engineering, the ability to separate and identify different biomolecules accurately and efficiently out of a complex biological sample is of utmost importance, for applications, such as proteomics and cancer diagnostics, as well as for understanding biomolecular signatures involved in human diseases [1–3]. In the new challenge of systems biology, one needs to separate and identify nucleic acids, proteins and other biologically relevant macromolecules from cell extracts or other complex biological fluids under many different physiological and pathological conditions [3]. Because of the large number of analytes involved, being able to automate the biomolecule analysis process so that it requires minimum human intervention is essential. None of the conventional separation technologies satisfies these requirements. Gel electrophoresis, gel-exclusion chromatography and other chromatography techniques used routinely for bioseparation are generally slow, difficult to automate and require large equipments [1,2]. Capillary electrophoresis is a fast analysis technique; however, it only separates biomolecules based on charge-to-size ratio and it therefore cannot analyze neutral biomolecules [4]. The microfluidic separation systems thus far have demonstrated much success in miniaturizing and automating biomolecule analysis processes [5–8]. However, most microfluidic separation systems adopt conventional polymeric gel materials as sieving media in their separation channels and these foreign sieving matrices pose intrinsic difficulties for integration of multi-step bioanalysis microsystems. Furthermore, these microchip systems are carried out as batch procedures and are therefore suited mainly for analytical bioseparation. This notable challenge poses the difficulty of harvesting purified biomolecules in quantities that are sufficient for downstream biosensing and detection [9].

The common, underlying problem of all conventional biomolecule separation and analysis techniques is a lack of engineering control in the molecular sieving and filtering process. For purification and separation of biomolecules, various kinds of nanoporous materials, such as polymeric gels and fibrous membranes, are used extensively as molecular sieving matrixes. These nanoporous materials consist of randomly distributed three-dimensional (3D) pore networks in which the sieving interactions with the migrating biomolecules determine the separation efficiency. These random materials provide nanometer-sized pores that are desirable for molecular sieving and filtering, although, by contrast, their random physical and chemical properties are difficult to control and manipulate. This prevents controlled experimental studies and hinders further process optimization. Over the past decade, there has been great interest in switching from disordered porous media to patterned regular sieving and filtering structures, in the hope of achieving a more efficient separation than achieved by polymeric gels and fibrous membranes with regard to separation speed and resolution [9–14]. A major goal of this review is therefore to offer a perspective on this new trend of designing artificial sieves and filters and their promise for biomolecule separation. We will first stress conceptual insights relating the working mechanisms behind the design of these artificial sieves and filters. In particular, we will review the relevant theoretical developments in the hindered transport theory and the sieving mechanisms in gel electrophoresis. Finally, we offer some speculations as to research directions and potential opportunities for new functionalities of artificial sieves and filters for bioseparation.

*Corresponding author:* Fu, J. (jianping.fu@alum.mit.edu).

0167-7799/$ – see front matter  doi:10.1016/j.tibtech.2008.02.009 Available online 20 April 2008

### Molecular sieving and filtering mechanisms

Transport properties of biomolecules through a sieving structure are determined mainly by the complex interplay between molecular dynamics in confined environments and nanofluidic physics, including physicochemical hydrodynamics [15–21]. Figure I in Box 1 depicts a simple example in which a spherical macromolecule migrates through a cylindrical nanopore. This scenario is of particular relevance to membrane separation and other related topics, such as ultrafiltration and gel-exclusion chromatography. The hydrodynamic theory for the hindered transport of rigid, spherical molecules in regular pores (such as cylinders and slits) has been well developed and the interrelated transport coefficients, such as partition coefficient, permeability and reflection coefficients, can be calculated from such fundamental information as the size, conformation and electrical charge of the solute macromolecules and the pores [1,17,18]. The situations for non-spherical and flexible macromolecules are more complex because the conformational dynamics of macromolecules within the nanopore can interplay with the physicochemical hydrodynamics to dominate their transport properties [16,17,22,23]. For concentrated solutions, the solute–solute interactions and the entanglement effect can become important, which will also affect their transport dynamics [16,17,24]. Other long-range solute–pore and solute–solute interactions can involve the electrostatic interactions [e.g. electric double layer (EDL) interaction, Van del Waals force], adsorption and desorption kinetics and polarization effect [17,25] (Box 1). For example, the EDL thickness can influence the molecular conformation, its persistence length or stiffness and its hydrodynamic and electrostatic screening lengths [26] and, therefore, affects the molecules' transport properties in the pore directly. This complex picture of a charged macromolecule migrating through the pore is not completed without also considering the coupled effects of the EDL and the physicochemical hydrodynamics, such as electrophoresis and osmosis or electro-osmosis on the solute–wall and solute–solvent interactions [27,28]; such strong coupling can in turn redirect the biomolecules for their energetically favored configurations and therefore affect their transport properties. Readers interested in further discussions in the hindered transport theory are referred to some excellent reviews published elsewhere [17,18].

The hindered transport theory can explain transport properties of biomolecules whose diameters are smaller than the sieve constriction size. However, complex conformational dynamics will start to dominate transport properties for cases in which the diameters of the molecules ($R_g$) are comparable or much greater than the constriction size ($\alpha$) [29,30] (Figure 1). The mechanistic concepts developed from gel electrophoresis and other related areas, such as polymer translocation through a nanopore, can help to

**Box 1. Hindered transport theory**

The partition coefficient $K$, defined as the equilibrium ratio of the configurational state integrals within the interstitial pore space to that in the bulk solution, is related directly to the entropic energy barrier $T\Delta S^0$ for partitioning from the bulk region to the confined space of the nanopore as $T\Delta S^0 = k_BT\ln(K)$ ($k_BT$: thermal energy) [1,15]. The partition coefficient $K$ can, in principle, be calculated from statistical thermodynamics as $K = \iiint p(r,\varphi,\lambda)drd\varphi d\lambda / \iiint drd\varphi d\lambda$. Generalized coordinates $r$, $\varphi$ and $\lambda$ describe molecular position, orientation and conformation, respectively, and $p(r,\varphi,\lambda)$ represents the probability density of the molecule having a given configuration $(r,\varphi,\lambda)$ within the pore space. The probability density $p(r,\varphi,\lambda)$ is a complex function of the solute–wall (steric and electrostatic effect) [15], solute–solute (solute concentration effect) [24] and solute–solvent (electrostatic effect, conformational dynamics and physicochemical hydrodynamic effects) interactions [22,23,25] (Figure I). For the simplest case of dilute rigid molecules with purely steric interaction, $p(r,\varphi,\lambda)$ is unity for all configurations in which the molecule does not overlap with the pore wall and is zero for forbidden configurations. This simplification reduces the calculation of $K$ to a geometric problem, in which $K$ is the ratio of the orientation-averaged pore volume available to the molecule center to total pore volume [15]. Using the hydrodynamic theory for the hindered transport of rigid, spherical molecules in cylindrical nanopores, the permeability coefficient $H$ and the reflection coefficient $\sigma_f$ can be calculated analytically as $H = K \times K_d$ and $\sigma_f = 1 - K \times K_c$, where $K_d$ and $K_c$ are two dimensionless factors that characterize the averaged intrapore molecule distribution. Detailed calculation for $K_d$ and $K_c$ an be found in Ref. [17].

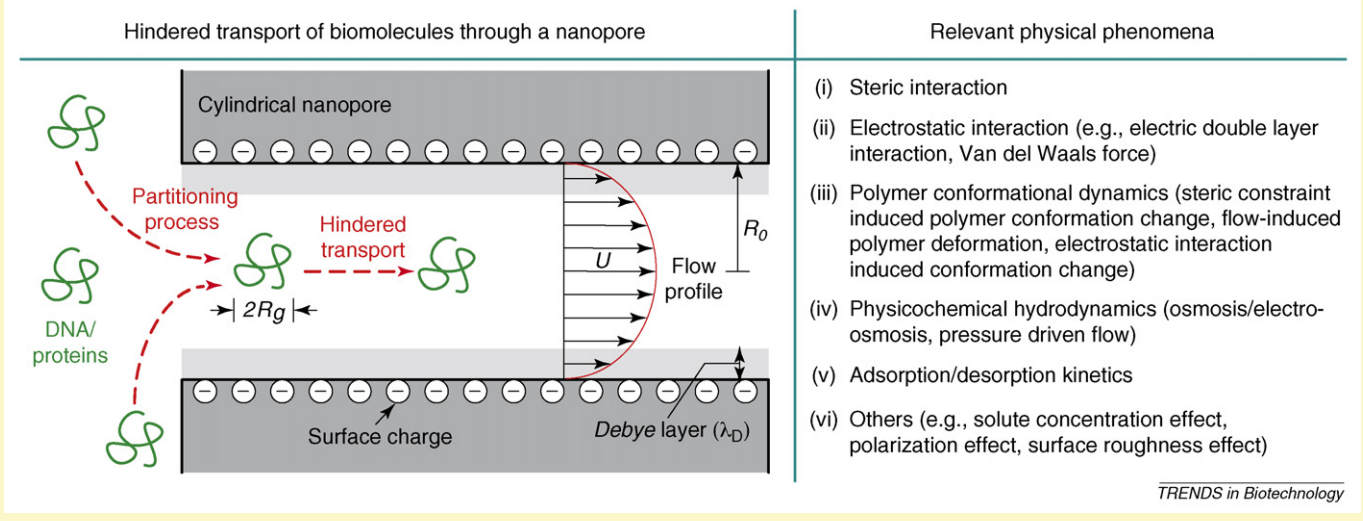


**Figure I**. Relevant physical phenomena involved in transport of charged macromolecules through a cylindrical nanopore.

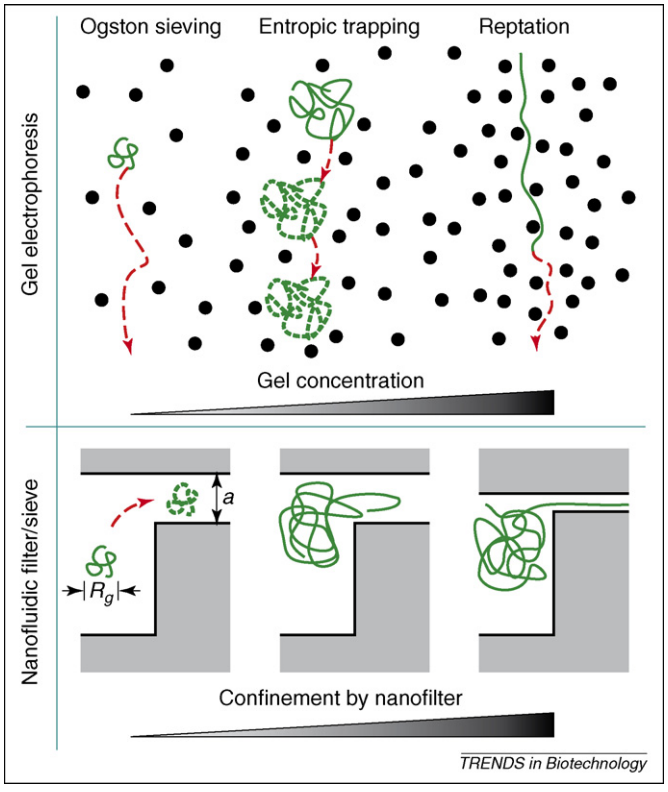


**Figure 1**. Different sieving regimes: gel electrophoresis (top) (reprinted, with permission, from Ref. [32]) versus artificial nanofluidic sieves and filters (bottom). Ogston sieving occurs because of steric interactions with the sieve structure (left). The entropic trapping transport applies when the conformation of the flexible macromolecule must deform to sneak through the sieve's spatial constrains (middle). Reptation can be envisioned as a long flexible macromolecule threading its way through the sieve in a snake-like fashion (top right). Translocation of charged biomolecules through a nanopore has been proposed as an efficient method for biosensing and DNA sequencing (bottom right) [24].

elucidate the complex conformational dynamics involved in such cases [28,31–35] (Box 2). For example, the entropic barrier-mediated transport has been identified in gel electrophoresis when $R_g/a > 1$, in which case the conformation of the flexible macromolecule must deform to pass through the gel [36,37]. The entropic trapping occurs because molecules spend most of their time in the larger pores and must therefore fight strong entropic forces to cross the narrow passages jointing these large and rare voids. For $R_g/a \gg 1$, the reptation regime starts to dictate gel electrophoresis [38,39]. Reptation can be envisioned as imposing lateral confinement on a diffusing linear macromolecule by enveloping the molecule in a fictitious tube. Transport of linear macromolecules through a nanopore also involves complex conformational changes and the interplay between polymer physics and physicochemical hydrodynamics [33,35]. As shown in Figure 1, the mechanistic picture of molecular sieving in artificial sieves and filters can be similar to the relevant situations in gel electrophoresis; however, it is worth mentioning that the theoretical results from gel electrophoresis are normally not applicable directly to artificial sieves and filters [29,40].

The relevant physical phenomena that dominate migration of charged biomolecules through sieving structures can be complex; however, these complex interactions and coupled physics can represent a valuable opportunity so that, by manipulating the *in situ* sieving process using artificial regular sieves and filters, more efficient separation can be achieved. One primary research direction in this area is the exploration of fundamental issues of molecular dynamics in confined environments and nanofluidic physics with the goal of discovering novel functionality in separation science. The development of novel functional artificial sieves and filters can be guaranteed if the mechanistics of the molecular interactions within sieving structures are well understood.

**Box 2. Sieving mechanisms in gel electrophoresis**

The separation mechanisms of gel electrophoresis are not yet understood fully at the microscopic level [28,31,32]. Depending on the relative size of the macromolecule compared with the gel mean pore size (e.g. the ratio of the radius of gyration $R_g$ of the molecule to the gel mean pore size $a$), three basic separation mechanisms have emerged to explain how flexible linear macromolecules migrate through a constraining gel medium – Ogston sieving ($R_g/a < 1$), entropic trapping ($R_g/a \sim 1$) and reptation ($R_g/a > 1$) (Figure 1). Which separation mechanism prevails under given conditions in gels remains an open question [32]. Sequential transitions from Ogston sieving to entropic trapping to reptation have been postulated as molecular weight or confinement increases. Such transitions, however, might not always be distinct.

**Ogston sieving**

In Ogston sieving, the macromolecule is smaller than the gel pores or constrictions and the molecular sieving occurs because of steric interactions of the macromolecules with the gel-pore network. Because $R_g/a < 1$, the molecules move rather freely through the gel matrix, assuming their unperturbed conformations. The concept of Ogston sieving has been studied extensively by Rodbard and Chrambach using Ogston's calculation for the pore-size distributions in random arrays of geometrically idealized obstacles (e.g. random planes, fibers) [28]. The Ogston sieving process has been suggested as an electric-field-driven partitioning process [28].

**Entropic trapping**

Entropic trapping applies when $R_g/a \sim 1$ and the conformation of the flexible macromolecule must deform or fluctuate to pass through the gel medium's spatial constrains. At each point, the number of accessible conformations defines the molecule's local entropy. Entropy differences derived from the gel medium's spatial heterogeneity drive molecules to partition or localize preferentially in less constrictive spaces, in which their enhanced conformational freedom raises entropy. Molecular transport then occurs by thermally activated jumps across the intervening entropic barriers. Entropic trapping in gel electrophoresis can also be regarded as an electric-field-driven partitioning process, but it involves deformation and conformational entropy penalty.

**Reptation**

Reptation can be envisioned as a long linear flexible macromolecule occupying multiple pores threading its way through the gel in a snake-like fashion, which is similar to the 'reptation in a tube' process originally proposed by de Gennes for entangled synthetic polymers [38]. In the reptation mechanism, only the end segments of the linear polymer chain can escape because the molecule undergoes random curvilinear motion along the tube axis. The tube's random contour and the molecule's sliding friction combine to hinder the center-of-mass displacement of the molecule. In contrast to the entropic-trapping transport, the number of configurations accessible to a reptating macromolecule does not depend on position.

## Artificial molecular sieves, filters and membranes

### *Artificial sieves and filters for bioseparation*

To the best of our knowledge, the first reported regular molecular sieve was composed of a capped array of

**Table 1. A summary of nanostructured artificial sieves, filters and membranes for bioseparation**

| Sieve design | Driving force | Separation mechanism | Biomolecule sample | Separation speed/rate | Refs |
|---|---|---|---|---|---|
| Asymmetric obstacle courses | Electric field | Rectified Brownian motion | DNA (15–30 kbp) | 2 μm/s | [42,43] |
| Entropic trap arrays | Electric field | Entropic trapping | DNA (5–160 kbp) | 15 μm/s | [44,45] |
| Micropillar array | Pulsed electric field | Electrophoretic stretching | DNA (61–209 kbp) | 10 ng/h | [47] |
| Nanopillar array | Electric field | Electrophoretic collision | DNA (1–38 kbp) | 15 μm/s | [49,50] |
| Micropillar array | Pressure | Bifurcation of laminar flow | DNA (60–200 kbp) | 100 pg/h | [51] |
| Nanofilter array | Electric field | Ogston sieving | DNA (50 bp-2 kbp); protein (10–200 kDa) | 20 μm/s | [52] |
| Anisotropic nanofilter array | Electric field | Ogston sieving, entropic trapping | DNA (50 bp-20 kbp); protein (10–300 kDa) | 30 μm/s | [53] |
| Self-assembled paramagnetic particle array | Electric field | Electrophoretic collision | DNA (15–145 kbp) | 3 μm/s | [55] |
| Porous alumina membrane | Electric field | Size-exclusion chromatography | DNA (0.3–3.2 kbp) | 30 μm/s | [57] |
| Self-assembled colloidal array | Electric field | Ogston sieving | DNA (0.05–50 kbp); protein (20–200 kDa) | 10 μm/s | [59] |
| Core-shell nanosphere media | Electric field | Ogston sieving | DNA (0.1–20 kbp) | 30 μm/s | [58] |
| Nuclear track-etched membrane | Electric field/Osmotic pressure | Hindered transport | Protein | 19 nmol/(cm$^2$ h) | [62] |
| Ultra-thin membrane | Osmotic pressure | Hindered transport | Protein (67–150 kDa) | 156 nmol/(cm$^2$ h) | [65,66] |

micrometer-sized pillars that were etched into a silicon wafer using conventional semiconductor microfabrication techniques [41]. Using such a pillar array, Austin and co-workers successfully observed *in situ* electrophoretic motion of highly stretched long DNA molecules. This provided an opportunity to observe sieving of flexible macromolecules directly in model molecular sieves with precisely known properties for the first time. Following on from this pioneering work, other groups have used various microfabrication techniques to fabricate microstructures or nanostructures as confining sieving matrix [42–52] (Table 1). So far, a wide range of regular sieve designs have been demonstrated with varying success in biomolecule separation. Examples include arrays of micrometer- or nanometer-sized pillars that mimic gel fibers [41,46–51], asymmetric obstacle courses that act as Brownian (thermal) ratchets [42,43] and microfluidic channels with alternating deep and shallow regions that form entropic traps [44,52]. The advantages of these microlithographically fabricated devices include precise control over the sieve geometry and the flexibility of the design depending on the desired application.

Regular array of micrometer- or nanometer-sized pillars have been fabricated using either contact photolithography (with pillar diameter and spacing down to 1 μm) [41,46,47,51] or e-beam photolithography (with pillar

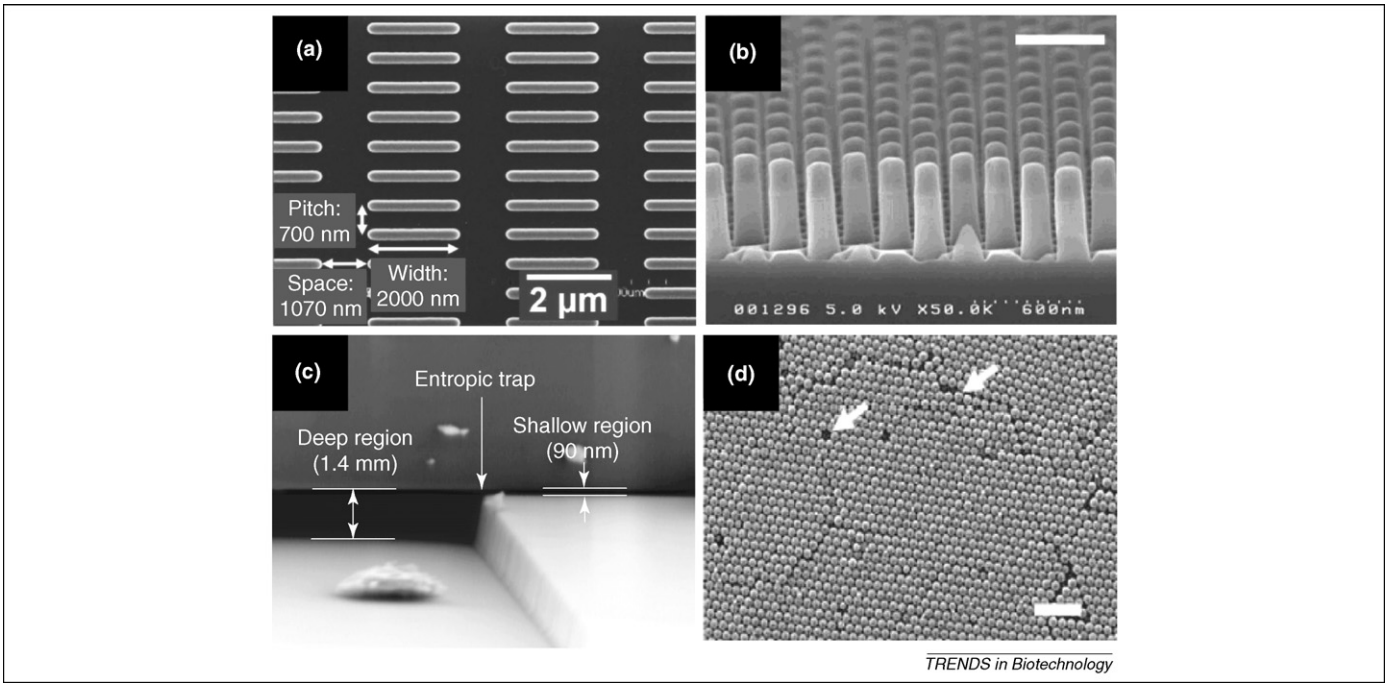


**Figure 2**. Artificial molecular sieves and filters for bioseparation. **(a)** Scanning-electron micrograph (SEM) of nano-obstacle arrays used for DNA separation. Reused, with permission, from Ref. [49]. Copyright (2003), American Institute of Physics. **(b)** Nanopillar structure for DNA separation. Scale bars: 500 nm. Reprinted in part, with permission, from Ref. [50]. Copyright (2004), American Chemical Society. **(c)** Entropic trap array with alternating deep (1.4 μm) and shallow (90 nm) regions. Reused, with permission, from Ref. [45]. Copyright (2001), Cornell University. **(d)** SEM image of a hexagonally closed packed 2-μm polystyrene colloidal array. The arrows indicate lattice defects. Scale bars: 10 μm. Reprinted in part, with permission, from Ref. [59]. Copyright (2004), American Chemical Society.

diameter or spacing down to 10 nm) [48–50] (Figure 2). A rapid separation of long DNA fragments [1–200 kilobase pairs (kbp)] has been demonstrated successfully both in a batch-separation mode [46,48–50] and in a continuous-flow fashion [47,51]. One notable example was the 'DNA Prism' devised by Huang *et al.* [47]. Using an asymmetrical pulse-field operation on fully stretched DNA molecules that were confined in the pillar array [much like in the conventional method of pulsed-field gel electrophoresis (PFGE)], the DNA Prism device was reported to separate long DNA fragments (61–209 kbp) continuously. The achieved separation speed was much faster than conventional PFGE and pulsed-field capillary electrophoresis. Another novel example using a nanometer-sized pillar array was based on the concept of entropic recoil [48]. Long DNA molecules were driven into the pillared area by electric field, whereby they became fully stretched. When the electric field was switched off, any DNA molecule resting entirely within the pillared area remained there, whereas those DNA molecules with segments extending outside the pillared area relaxed back and recoiled to maximize their conformational entropy. Because shorter DNA molecules were more likely to be driven entirely into the pillared area, they would not recoil back and therefore their effective mobility in the device was greater. This entropic recoil device had been reported for the separation of T2 (167 kbp) and T7 (39 kbp) phage DNA within a few minutes [48].

Han and Craighead designed an entropy-based separation system in which a microfluidic channel was defined by a sequence of deep and shallow channels [44,45] (Figure 2c). For long DNA molecules with diameters greater than the shallow region constriction size, passage requires the DNA molecule to deform and form hernias at the cost of internal conformational entropy. Interestingly, longer DNA molecules advance faster than shorter ones across the entropic barriers [29]. This counter-intuitive observation could be owing to longer DNA molecules having a larger surface area contacting the constriction and thus a greater probability to form hernias, which initiate the escape process. Han and Craighead could apply this entropy-based system to separate long DNA ladder samples (5–50 kbp) in approximately 30 min [44].

Recently, Fu *et al.* developed a one-dimensional (1D) nanofilter array system that extended separation with regular sieving structures to physiologically relevant macromolecules, such as shorter DNA molecules (50 bp–2 kbp) and proteins (10–200 kDa) [52] (Figure 3). The design of the 1D nanofilter array device was similar to the entropic trap array; however, separation of the biomolecules was based on Ogston sieving. In the nanofilter array, the limited configurational freedom inside the nanofilter shallow region created a size-dependent configurational entropic barrier for the molecule passage from the deep region to the confined space of the nanofilter, a partitioning process similar to the hindered transport at the nanopore entrance (Figure 3a–b); therefore, smaller biomolecules jump faster across the nanofilter constriction. The speed and resolution reported by the authors was comparable to other state of the art systems (i.e. capillary gel electrophoresis) [7]. The fabrication strategy for the nanofilter array device enables further increasing of the

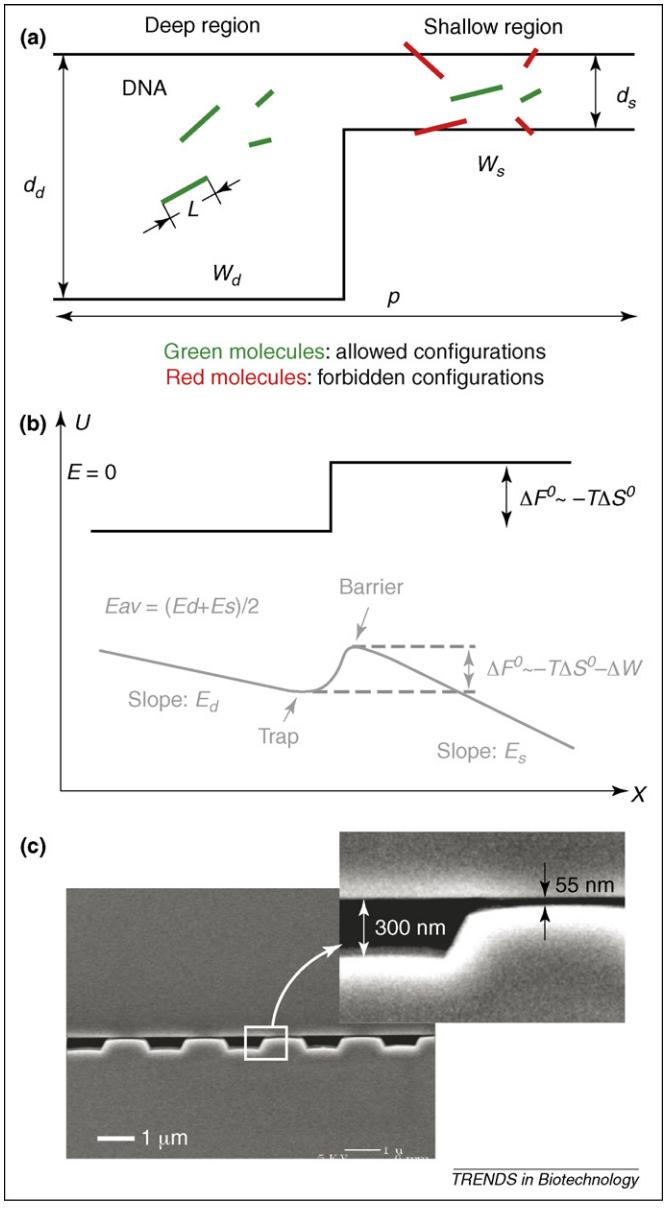


**Figure 3.** **(a)** Partitioning of rigid, rod-like DNA across a nanofilter that consists of a deep region and a shallow region. **(b)** Free energy landscapes experienced by DNA while crossing a nanofilter. **(c)** SEM images of alternating deep (300 nm) and shallow (55 nm) regions of the nanofilter array. Reprinted, with permission, from Ref. [40]. Copyright (2006) by the American Physical Society.

nanofilter density and decreasing of the nanofilter gap size, leading, in principle, to even faster separation. More recently, Fu *et al.* further devised a two-dimensional (2D) anisotropic nanofilter array (ANA) that sorted DNA and proteins continuously within a few minutes, covering broad size ranges (DNA: 50 bp–23 kbp; protein: 10–400 kDa) [53]. The designed structural anisotropy in the ANA caused macromolecules with different sizes or charges to follow distinct trajectories, leading to an efficient separation (Box 3). The ANA also represents a significant advance compared with the authors' earlier work in 1D nanofilter arrays because the continuous-flow operation of the ANA permits continuous harvesting of the subset of biomolecules of interest to enhance the specificity and sensitivity for downstream biosensing and detection, which is highly desirable for integrated bioanalysis micro-

## Box 3. Anisotropic sieving structures for continuous-flow bioseparation

The structural anisotropy in a 2D sieving medium can cause biomolecules of different properties (e.g. size, charge or hydrophobicity) to follow distinct migration trajectories, leading to efficient separation. The stream deflection angle $\theta$ in a 2D medium can be calculated as $\tan\theta = V_x/V_y = (\mu_x/\mu_y) \times (E_x/E_y)$, where $V$ and $E$ are the migration velocity and electric field, respectively, and the subscripts $x$ and $y$ denote the two orthogonal axis of the 2D medium. In an isotropic medium, the mobility $\mu$ is isotropic; thus, $\mu_x$ equals $\mu_y$, leading to $\tan\theta = E_x/E_y$ (Figure Ia, left). Therefore, the stream-defection angle $\theta$ in an isotropic medium is determined solely by $E_x$ and $E_y$ and different biomolecules follow the same trajectory without separation. In an anisotropic medium, $\mu_x/\mu_y$ becomes a complex function of both the sieve structural anisotropy and molecular properties and $\tan\theta = (\mu_x/\mu_y) \times (E_x/E_y) = f(\text{size, charge, etc.}) \times (E_x/E_y)$. Thus, different biomolecules will have a different stream-deflection angle $\theta$, leading to separation (Figure Ia, right).

Figure Ib shows an example of the anisotropic sieving structure design, called the anisotropic nanofilter array (ANA). The design of the ANA consists of a 2D periodic nanofilter array. The separation mechanism of the ANA relies on different sieving characteristics along two orthogonal directions within the ANA, which are set perpendicular and parallel to the nanofilter rows. On application of an electric field $E_y$ along the positive $y$-axis, uniformly negative-charged molecules (such as DNA) injected into the array assume a drift motion in deep channels with a negative velocity $V_y$ that is size independent. An orthogonal electric field $E_x$ is superimposed along the negative $x$-axis across the nanofilters and this field drives the drifting molecules in the deep channel selectively to jump across the nanofilter in the positive $x$-direction to the adjacent deep channel. Molecular crossings of the nanofilter under the influence of the electric field $E_x$ can be described as biased thermally activated jumps across free energy barriers at the nanofilter threshold [29,40]. For Ogston sieving, this energy barrier favors molecules with a smaller size for passage [40] (Figure Ib, left), resulting in a greater jump passage rate $P_x$ for shorter molecules. Therefore, shorter molecules exercise a shorter mean characteristic drift distance $L$ in the deep channels between two consecutive nanofilter crossings, leading to a larger stream deflection angle $\theta$. For molecules with diameters greater than the nanofilter constriction size, passage requires the molecules to deform and form hernias at the cost of their internal conformational entropy (i.e. entropic trapping). Longer molecules have a higher escape-attempt frequency and therefore assume a greater jump-passage rate $P_x$ [29], resulting in a larger deflection angle $\theta$.

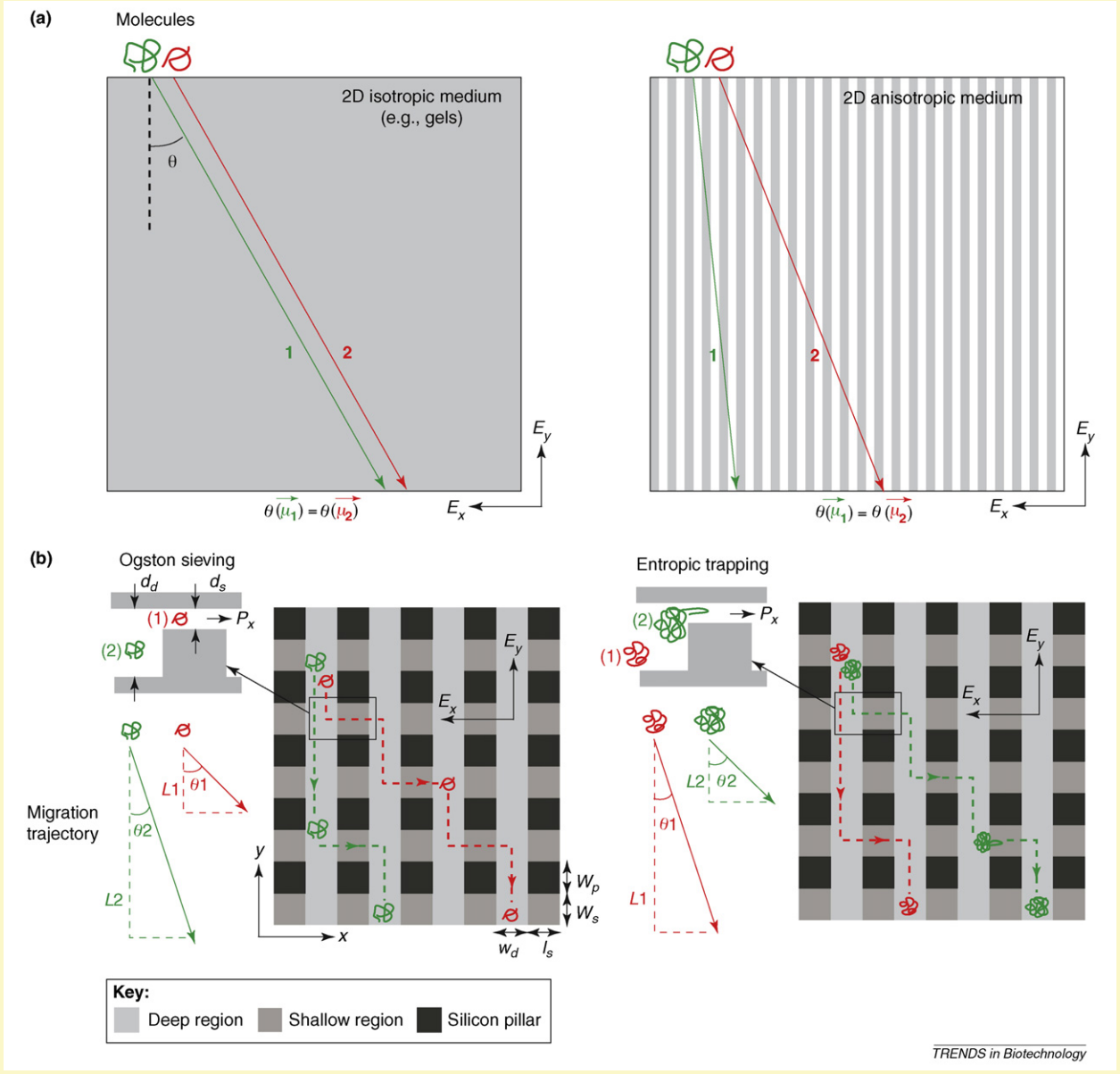


**Figure I**. Anisotropic sieving structures for continuous-flow biomolecule separation. Part **(b)** is reprinted by permission from Macmillan Publishers Ltd: *Nature Nanotechnology*, Ref. [53], copyright (2007).

systems because of the low sample throughput [9,14,54]. This continuous-flow separation through the ANA is also believed to be applicable to any interaction mechanism (size, charge or hydrophobicity based) along the orthogonal sieving direction that can lead to differential transport across the nanofilters [14,53,54]. The high-resolution separation and ease of sample collection might prove useful for preparative separation of complex biological samples, which has promising implications for proteomic research and biomarker discovery.

Other novel approaches for the construction of artificial molecular sieves have also been reported. Doyle *et al.* constructed column-like microstructures by applying a homogeneous magnetic field to a suspension of superparamagnetic particles that were contained in microfluidic channels [55]. By varying channel size and particle concentration, the column spacing can be tuned from submicrometer to approximately 100 μm [56]. Therefore, this method provided an additional tunability of the sieving structure (or sieve pore size) after device construction, a feature that is not possible with microlithography techniques. Doyle *et al.* separated digestion products of λ-phage DNA successfully in approximately 10 min [55]. Recently, Sano *et al.* reported a size-exclusion chromatography device that used anodic porous alumina confined in a microfluidic channel as the separation matrix [57]. The porous alumina membrane trapped smaller biomolecules more frequently and they therefore eluted more slowly than the larger biomolecules in the channel. This porous alumina membrane had a uniform nanoscale pore distribution and the fabrication of this membrane was relatively easy and inexpensive because it did not require nanolithography tools. Tabuchi *et al.* reported another novel technology that used a core-shell-type nanosphere and nanoparticle medium on a microchip format to separate a wide range of DNA fragments (100 bp–20 kbp) with high speed and high resolution [58]. A recent exciting development by Zeng and Harrison used self-assembled silica bead arrays confined in microfluidic channels as the sieving matrix to separate both DNA and proteins with high resolution [59]. The flexibility of the tunable pore size enabled by their method (by using silica beads of different sizes) provided separation of biomolecules with a wide size distribution ranging, for proteins, from 20 to 200 kDa and, for DNA, from 0.05 to 50 kbp. To our knowledge, this is the first demonstration of size separation of biomolecules within self-assembled ordered colloidal lattices.

### *Artificial membranes for bioseparation*

Nuclear track-etched membrane (NTE membrane) was one of the first artificial membranes used for bioseparation and its development dates back to the early 1970s [60]. NTE membranes are generated by irradiation of plastic films [polycarbonate (PC) or polyethylene terephthalate (PET)] with a high energetic beam of heavy-fission fragments. The energetic particles produce damage tracks in the material and enable a highly directional subsequent chemical etching (Figure 4a). Pore-number density and pore radius are controlled by the particle dose and etching conditions, respectively, and, therefore, can be varied independently. Pore radii as small as 3 nm have been achieved [60]. The shape of the resulting pore can be manipulated to a lesser degree; however, truly cylindrical or conical pores as well as highly parallel pores with desired angles relative to the membrane surface have been demonstrated [60]. Several surface-modification methods have been applied to change the pore surface and therefore impart new functionality to NTE membranes. Examples include hydrophilization [60] and layer-by-layer deposition of polyelectrolyte multilayers in NTE membrane pores [61]. A recent development that used NTE membranes as a template could be applied to various bioseparations. Martin and his co-workers fabricated Au nanotubule membranes with controlled inside diameters that approached truly molecular dimensions (<1 nm) by electroless gold plating onto the walls of NTE membrane pores [62]. These unique Au nanotubule membranes could separate pyridine [molecular weight (MW): 79] and quinine (MW: 324) successfully, with a selectivity that was greater than with conventional dialysis membranes. Recently, Shannon and his co-workers sandwiched NTE membranes between two polydimethylsiloxane (PDMS) microfluidic channels, thereby developing a multilayered microfluidic separation system that exhibited a protein-separation cutoff of approximately 10 kDa with a NTE membrane pore size of 15 nm [63].

Artificial membranes with pores in the nanometer scale can also be fabricated with conventional semiconductor microfabrication techniques. Létant *et al.* fabricated nanochannel arrays with diameters down to 30 nm, in a silicon membrane that was 8 μm thick, by combining conventional microfabrication techniques with electrochemical breakdown etching [64] (Figure 4c). Their technique was fast, reproducible and inexpensive and was able to produce membranes with extremely parallel nanopores. However, this class of micrometer-thick membranes, although robust mechanically, can lead to a high transmembrane-pressure drop, which results in a high flow resistance and, consequently, a low sample throughput. A recent development of artificial membranes was the ultra-thin silicon nitride (SiN) membrane, the thickness of which became comparable to or even smaller than the pore diameters. Using focused ion beam (FIB) drilling, Tong *et al.* produced an ultra-thin SiN membrane with a thickness of 10 nm and a uniform cylindrical pore diameter of 25 nm [65] (Figure 4d). This SiN nanofluidic membrane possesses mechanical strength up to several bars of transmembrane pressure over a $50 \times 50\ \mu m^2$ area. A more recent exciting development of a relatively inexpensive ultra-thin porous membrane had been demonstrated by Striemer *et al.* [66] (Figure 4e). Using standard microfabrication techniques, the authors of this study were able to fabricate a 15-nm-thick porous nanocrystalline silicon (pnc-Si) membrane with a narrow pore size distribution and a well defined average pore size that ranged from 5 to 25 nm. A $200 \times 200\ \mu m^2$ pnc-Si membrane sustained several bars of transmembrane pressure without fracturing and separated albumin (MW: 67 kDa) and immunoglobulin G (MW: 150 kDa) efficiently. This pnc-Si membrane showed a much higher selectivity than conventional nanoporous polymer

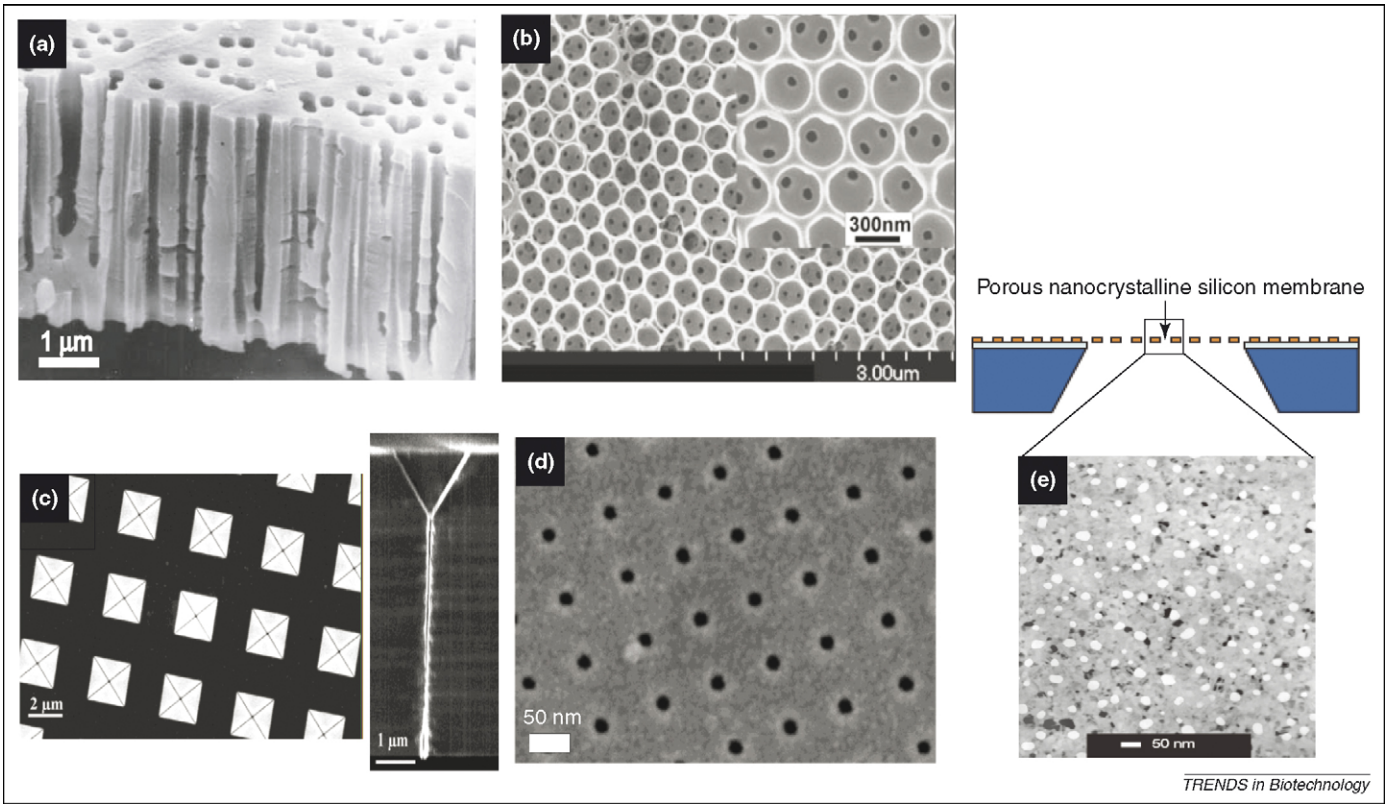


**Figure 4**. Artificial membrane filters for bioseparation. **(a)** Track-etched membrane with slightly conical parallel pores. Reprinted, with permission, from Ref. [60]. **(b)** Membranes prepared with 334 nm silica particles by colloidal self-assembly. Reprinted, with permission, from Ref. [67]. Copyright Wiley-VCH Verlag Gmbh & Co. KGaA. **(c)** SEM micrographs of a nanochannel membrane with a pore diameter of 30 nm and a thickness of 8 μm fabricated by electrochemistry. Top view (left) and cross-section view (right). Reprinted in part, with permission, from Ref. [64]. Copyright (2004), American Chemical Society. **(d)** A 10-nm-thick SiN membrane with a pore size of 25 nm fabricated by focused ion beam. Reprinted in part, with permission, from Ref. [65]. Copyright (2004), American Chemical Society. **(e)** Transmission-electron microscope (TEM) image of a 15-nm-thick pnc-Si membranes. Pores appear as bright spots whereas nanocrystalline silicon is in gray or black color. Reprinted by permission from Macmillan Publishers Ltd: *Nature*, Ref. [66], copyright (2007).

membranes, which normally require a size difference of 10-fold for effective separation [2].

## Conclusions

One of the key parameters for efficient bioseparation is the separation selectivity and resolution. Currently, significant efforts are devoted toward developing artificial sieves with improved separation resolution [52,58,59]. It is of great interest to further pursue this research direction by designing artificial sieves with increasingly elaborate geometries, while at the same time investigating novel separation functionalities. It is possible to design a molecular sieving structure with heightened size selectivity and a bias toward limited band broadening to enhance separation resolution [51,53]. In addition to applications in biomolecule separation, artificial sieving structures, with their precisely characterized environments, are ideal tools for theoretical studies of molecular dynamics and stochastic motion in confining spaces [9–15]. In particular, studies of jump dynamics of biomolecules with effective diameters smaller than the sieve constriction size (such as occurring during Ogston sieving) have great impact on the design of future artificial sieves for the rapid separation of proteins, carbohydrates and hormones [14,40]. Such investigations and characterization could potentially aid in developing cheaper and more accurate medical screening and diagnostic devices. Because the size selectively of a nanopore can be enhanced by decreasing the pore radius [14,40], it would be of great interest to further improve separation efficiency of the so-far demonstrated artificial molecular sieves and filters by scaling down their structural parameters, including the pore size, with advanced photolithography techniques and other available tools.

Surface modification of artificial sieving structures has the potential to add unique functionalities for bioseparation. For example, tailored surface functionalities have been achieved with modified surface-charge density and hydrophobicity [60,61]. Incorporating gate electrodes on the sieve walls can enable additional active control of the surface potential, thus introducing a new degree of control to enhance the electrostatic interaction across the sieve and filter channel [68,69]. It would be interesting to use the EDL, electro-osmosis and surface chemistries, together with the geometrical constraints inherent to the sieve, to achieve novel biomolecule separation based on an entire array of molecular properties, such as size, charge or hydrophobicity. The amount of sample separated using artificial sieves and filters is another important practical concern that is especially crucial for sample preparation [9,14]. The recent development of different continuous-flow separation systems (e.g. ANA), as well as the application of ultra-thin nanopore membranes, has begun to show some promising solutions [66,70]. However, before further advances in large-scale bioseparations are possible, a convenient and inexpensive method to fabricate robust molecular sieves and membrane filters with highly parallel

nanopores will need to be developed. We believe this is a major challenge for the near future.

In summary, the development of artificial sieving structures represents a major step towards optimizing biomolecule separation methods and integrating them within other bioanalysis systems. The design flexibility and the precise control over geometries within artificial sieves constitute key advantages offered by regular sieve structures compared with conventional random gel-based sieving media. Further development of artificial molecular sieves and filters with more elaborate geometrical constraints and tailored surface functionality is believed to further provide promising results for bioseparation. In addition, coupling of the fundamental physics of molecular dynamics in confined environments and nanofluidic physics with artificial molecular-sieve design could provide an additional opportunity to exploit such coupling for the discovery of novel functionality in separation science.

**Acknowledgements**

The authors are grateful for financial support from National Institutes of Health (EB005743), National Science Foundation (CTS-0347348), Singapore-MIT Alliance (SMA-II, CE program) and KIST-IMC (Intelligent Microsystems Center). The valuable input from all the members in the Micro/Nanofluidic BioMEMS Group at MIT is greatly appreciated. Finally, we extend our apologies to all our colleagues in the field whose work we were unable to cite formally because of imposed reference limitations.

**References**

1 Giddings, J.C. (1965) *Dynamics of chromatography: principles and theory part 1,* Marcel Dekker
2 Scopes, R.K. (1993) *Protein purification: principles and practice* (3rd edn), Springer-Verlag
3 Smejkal, G.B. and Lazarev, A., eds (2006) *Separation methods in proteomics*, CRC Taylor and Francis
4 Camilleri, P. (ed.) (1998) *Capillary electrophoresis: theory and practice*, CRC Press
5 Wehr, T. *et al.* (2001) In *Capillary Electrophoresis of Nucleic Acids: Introduction to the Capillary Electrophoresis of Nucleic Acids* (Vol. 1) (Mitchelson K.R. and Cheng, J., eds), pp. 167–187, Humana Press
6 Viovy, J.L. and Dukc, T. (1993) DNA electrophoresis in polymer solutions: ogston sieving, reptation and constraint release. *Electrophoresis* 14, 322–329
7 Yao, S. *et al.* (1999) SDS capillary gel electrophoresis of proteins in microfabricated channels. *Proc. Natl. Acad. Sci. U. S. A.* 96, 5372–5377
8 Callewaert, N. *et al.* (2004) Total serum protein N-glycome profiling on a capillary electrophoresis-microfluidics platform. *Electrophoresis* 25, 3128–3131
9 Eijkel, J.C. and van den Berg, A. (2006) Nanotechnology for membranes, filters and sieves. A series of mini-reviews covering new trends in fundamental and applied research, and potential applications of miniaturised technologies. *Lab Chip* 6, 19–23
10 Chou, C-F. *et al.* (2000) Sorting biomolecules with microdevices. *Electrophoresis* 21, 81–90
11 Tegenfeldt, J.O. *et al.* (2004) Micro-and nanofluidics for DNA analysis. *Anal. Bioanal. Chem.* 378, 1678–1692
12 Eijkel, J.C.T. and Berg, A. (2005) Nanofluidics: what is it and what can we expect from it? Microfluid. *Nanofluid.* 1, 249–267
13 Craighead, H. (2006) Future lab-on-a-chip technologies for interrogating individual molecules. *Nature* 442, 387–393
14 Han, J. *et al.* (2008) Molecular sieving using nanofilters: past, present and future. *Lab Chip* 8, 23–33
15 Giddings, J.C. *et al.* (1968) Statistical theory for the equilibrium distribution of rigid molecules in inert porous networks. Exclusion chromatography. *J. Phys. Chem.* 72, 4397–4408
16 DeGennes, P.G. (1979) *Scaling Concepts in Polymer Physics,* Cornell University Press
17 Deen, W.M. (1987) Hindered transport of large molecules in liquid-filled pores. *AIChE J.* 33, 1409–1425
18 Kulkarni, S.S. *et al.* (1992) Ultrafiltration: theory and mechanistic concepts. In *Membrane Handbook* (Ho, W.S. and Sirkar, K.K., eds), p. 398, Van Nostrand Reinhold
19 Grosberg, A.Y. and Khokhlov, A.R. (1994) *Statistical Physics of Macromolecules,* AIP Press
20 Probstein, R.F. (1994) *Physicochemical Hydrodynamics: An Introduction,* John Wiley & Sons
21 Baldessari, F. and Santiago, J.G. (2006) Electrophoresis in nanochannels: brief review and speculation. *J. Nanobiotechnol.* 4, 12
22 Casassa, E.F. (1967) Equilibrium distribution of flexible polymer chains between a macroscopic solution phase and small voids. *J. Polym. Sci.* 5, 773–778
23 White, J.A. and Deen, W.M. (2000) Equilibrium partitioning of flexible macromolecules in fibrous membranes and gels. *Macromolecules* 33, 8504–8511
24 White, J.A. and Deen, W.M. (2001) Effects of solute concentration on equilibrium partitioning of flexible macromolecules in fibrous membranes and gels. *Macromolecules* 34, 8278–8285
25 Smith, F.G. and Deen, W.M. (1983) Electrostatic effects on the partitioning of spherical colloids between dilute bulk solution and cylindrical pores. *J. Colloid Interface Sci.* 91, 571–590
26 Hagerman, P.J. (1988) Flexibility of DNA. *Annu. Rev. Biophys. Biophys. Chem.* 17, 265–286
27 Long, D. *et al.* (1996) Simultaneous action of electric fields and nonelectric forces on a polyelectrolyte: motion and deformation. *Phys. Rev. Lett.* 76, 3858–3861
28 Viovy, J-L. (2000) Electrophoresis of DNA and other polyelectrolytes: physical mechanisms. *Rev. Mod. Phys.* 72, 813–872
29 Han, J. *et al.* (1999) Entropic trapping and escape of long DNA molecules at submicron size constriction. *Phys. Rev. Lett.* 83, 1688–1691
30 Nykypanchuk, D. *et al.* (2002) Brownian motion of DNA confined within a two-dimensional array. *Science* 297, 987–990
31 Kozulic, B. (1995) Models of gel electrophoresis. *Anal. Biochem.* 231, 1–12
32 Slater, G.W. *et al.* (1996) Migration of DNA through gels. *Methods Enzymol.* 270, 272–295
33 de Gennes, P.G. (1999) Passive entry of a DNA molecule into a small pore. *Proc. Natl. Acad. Sci. U. S. A.* 96, 7262–7264
34 Deamer, D.W. and Branton, D. (2002) Characterization of nucleic acids by nanopore analysis. *Acc. Chem. Res.* 35, 817–825
35 Muthukumar, M. (2007) Mechanism of DNA transport through pores. *Annu. Rev. Biophys. Biomol. Struct.* 36, 435–450
36 Muthukumar, M. and Baumgärtner, A. (1989) Effects of entropic barriers on polymer dynamics. *Macromolecules* 22, 1937–1941
37 Rousseau, J. *et al.* (1997) Entropic trapping of DNA during gel electrophoresis: effect of field intensity and gel concentration. *Phys. Rev. Lett.* 79, 1945–1948
38 de Gennes, P.G. (1971) Reptation of a polymer chain in the presence of fixed obstacles. *J. Chem. Phys.* 55, 572–579
39 Slater, G.W. and Noolandi, J. (1986) On the reptation theory of gel electrophoresis. *Biopolymers* 25, 431–454
40 Fu, J. *et al.* (2006) Molecular sieving in periodic free-energy landscapes created by patterned nanofilter arrays. *Phys. Rev. Lett.* 97, 018103
41 Volkmuth, W.D. and Austin, R.H. (1992) DNA electrophoresis in microlithographic arrays. *Nature* 358, 600–602
42 Chou, C.F. *et al.* (1999) Sorting by diffusion: an asymmetric obstacle course for continuous molecular separation. *Proc. Natl. Acad. Sci. U. S. A.* 96, 13762–13765
43 van Oudenaarden, A. and Boxer, S.G. (1999) Brownian ratchets: molecular separation in lipid bilayers supported on patterned arrays. *Science* 285, 1046–1048
44 Han, J. and Craighead, H.G. (2000) Separation of long DNA molecules in a microfabricated entropic trap array. *Science* 288, 1026–1029
45 Han. J. (2001) Entropic trap array device for DNA separation. Ph.D. thesis, Cornell University
46 Bakajin, O. *et al.* (2001) Separation of 100-kilobase DNA molecules in 10 seconds. *Anal. Chem.* 73, 6053–6056
47 Huang, L.R. *et al.* (2002) A DNA prism: high speed continuous fractionation of large DNA molecules. *Nat. Biotechnol.* 20, 1048–1051
48 Cabodi, M. *et al.* (2002) Entropic recoil separation of long DNA molecules. *Anal. Chem.* 74, 5169–5174

49 Baba, M. *et al.* (2003) DNA size separation using artificially nanostructured matrix. *Appl. Phys. Lett.* 83, 1468–1470
50 Kaji, N. *et al.* (2004) Separation of long DNA molecules by quartz nanopillar chips under a direct current electric field. *Anal. Chem.* 76, 15–22
51 Huang, L.R. *et al.* (2004) Continuous particle separation through deterministic lateral displacement. *Science* 304, 987–990
52 Fu, J. *et al.* (2005) Nanofilter array chip for fast gel-free biomolecule separation. *Appl. Phys. Lett.* 87, 263902
53 Fu, J. *et al.* (2006) A patterned anisotropic nanofluidic sieving structure for continuous-flow separation of DNA and proteins. *Nature Nanotechnol.* 2, 121–128
54 Austin, R. (2006) Nanofluidics: a fork in the nano-road. *Nature Nanotechnol. 2* 121–128
55 Doyle, P.S. *et al.* (2002) Self-assembled magnetic matrices for DNA separation chips. *Science* 295, 2237
56 Liu, J. *et al.* (1995) Field-induced structures in ferrofluid emulsions. *Phys. Rev. Lett.* 74, 2828–2831
57 Sano, T. *et al.* (2003) Size-exclusion chromatography using self-organized nanopores in anodic porous alumina. *Appl. Phys. Lett.* 83, 4438–4440
58 Tabuchi, M. *et al.* (2004) Nanospheres for DNA separation chips. *Nat. Biotechnol.* 22, 337–340
59 Zeng, Y. and Harrison, D.J. (2007) Self-assembled colloidal arrays as three-dimensional nanofluidic sieves for separation of biomolecules on microchips. *Anal. Chem.* 79, 2289–2295
60 Apel, P. (2001) Track etching technique in membrane technology. *Radiat. Meas.* 34, 559–566
61 Alem, H. *et al.* (2007) Layer-by-layer assembly of polyelectrolytes in nanopores. *Macromolecules* 40, 3366–3372
62 Jirage, K.B. *et al.* (1997) Nanotubule-based molecular-filtration membranes. *Science* 278, 655–658
63 Kuo, T-C. *et al.* (2003) Gateable nanofluidic interconnects for multilayered microfluidic separation systems. *Anal. Chem.* 75, 1861–1865
64 Létant, S.E. *et al.* (2004) Nanochannel arrays on silicon platforms by electrochemistry. *Nano Lett.* 4, 1705–1707
65 Tong, H.D. *et al.* (2004) Silicon nitride nanosieve membrane. *Nano Lett.* 4, 283–287
66 Striemer, C.C. *et al.* (2007) Charge- and size-based separation of macromolecules using ultrathin silicon membranes. *Nature* 445, 749–753
67 Yan, F. and Goedel, W.A. (2004) A simple and effective method for the preparation of porous membranes with three-dimensionally arranged pores. *Adv. Mater.* 16, 911–915
68 Schasfoort, R.B. *et al.* (1999) Field-effect flow control for microfabricated fluidic networks. *Science* 286, 942–945
69 Karnik, R. *et al.* (2006) Field-effect control of protein transport in a nanofluidic transistor circuit. *Appl. Phys. Lett.* 88, 123114
70 Pamme, N. (2007) Continuous flow separations in microfluidic devices. *Lab Chip* 7, 1644–1659